Fiber distribution in a 3D FEM Model of the Supraspinatus Tendon

Author:
Romy Hasler

Supervisors:
Christoph Engelhardt
Alexandre Terrier
Dominique Pioletti

June 6, 2014

Abstract

The supraspinatus tendon is often involved in rotator cuff tears. The pathogenesis of such tears is not well known and can be multicausal (mechanical, inflammatory, ...). The idea of this project was to analyse the mechanical contribution to rotator cuff tears with a numerical deformation analysis of the supraspinatus tendon.

The tendon was simulated under tension in two conditions: an isotropic case and an anisotropic case. In the isotropic case, the tendon was simulated with the same material properties in every direction. In the anisotropic case, the tendon's fiber were computed and the material was defined in the fiber direction and in the transverse direction.

In the isotropic case, the strain was found to be higher in the two studied position (90 ° abduction and rest position) than in the anisotropic case. In both cases (isotropic and anisotropic) the maximal strain is situated at the distal side of the tendon insertion on the humeral head. The difference in the strain value is due to the fact that the isotropic material definition is averaged in all direction and therefore is softer in the fiber direction and stronger in the transverse direction. The isotropic model is therefore not very consistant with a real tendon structure. Both models are consistent with clinical observations as supraspinatus tears occur usually at the distal side of the insertion. However, for qualitative deformation analysis an anisotropic material choice is recommended.

Acknowledgements

I would like to thank Christoph Engelhardt, first for giving me the possibility to work on this project, and then for all his support and guidance along it. I'm grateful for all the new things I could learn and for all the time you consecrated to me to lead this project to the end.
I'd also like to thank Alexandre Terrier for his interest in my project and for his guidance to the conclusion of the project.

Contents

1 Introduction

The shoulder articulation is made of three bones (the scapula, the humerus and the clavicle) which are connected by muscles and ligaments. The shoulder joint has the greater range of motion of all joints in the body and must therefore be stabilised without loss of mobility. The stability of the shoulder is given by ligaments and by the rotator cuff muscles. The muscles of the rotator cuff includes the supraspinatus, the teres minor, the infraspinatus and the subscapularis muscles. As these muscles play an important role in the stability of the shoulder, they are under a lot of constrain. This result that they are often implied in shoulder pathologies like rotator cuff tears. The tendon of the supraspinatus muscle is the tendon out of the rotator cuff muscles which is the most often affected by tears, but the pathogenesis of the rotator cuff tears is unclear. In fact, there are several supposed causes for pathologies but most of them are not proven to be resulting in a specific pathology. These causes can for exemple be mechanical or inflammatory.

Therefore, to better understand the supraspinatus muscle and its interaction with the surrounding bones, 3D models are created to simulate the muscle in its environment. These numerical models allow to predict the deformation of structures under applied loads and therefore allows to analyse the mechanical contribution to supraspinatus tear.

In previous studies, the muscle has been well studied but the tendon was most of the time considered as isotropic. This means that the material definition of the tendon was defined to be the same in all direction. Therefore, this method doesn't consider the fibrous structure of the tendon. The aim of this project was to analyse the deformation of the supraspinatus tendon and to compare isotropic vs anisotropic modelling techniques of the tendon tissue.

To do so, first the fiber direction was implemented in the supraspinatus tendon in a three dimensional model. Then different simulations, applying the material definition and a force, could be made on the models. This allowed a comparison between an isotropic model and an anisotropic model.

2 State of the art

2.1 Anatomy

All the anatomic informations were take from Netter (2011), Wikipedia (2014) and Marieb (2005)

2.1.1 Shoulder

In figure 2.1 the shoulder anatomy is shown. The shoulder articulation is made of three paires of bones (left and right symmetry): the scapula, the humerus and the clavicle, which are connected by the sternum in the middle. These bones are bound together by muscles, their tendons and ligaments.
There are three joints between the bones: the acromioclavicular joint between the acromion of the scapula and the clavicle; the sternoclavicular joint between the sternum and the clavicle; and the glenohumeral joint between the glenoid cavity of the scapula and the head of the humerus.
The acromioclavicular articulation has only one degree of freedom, which allows to raise the arm above the head. The sternoclavicular articulation has three degree of freedom and is stabilised by ligaments. The glenohumeral joint has three degree of freedom allowing the arm to move in the vertical and horizontal as well as rotated about its longitudinal axis.

2.1.2 Shoulder Muscles

The shoulder movements are very complexe due to the large range of motion and high degree of freedom of the articulation. These movements are assured by a large number of muscles. The main muscles used to articulate the glenohumeral joint are:

- the deltoid muscles (anterior, middle and posterior) which arise from the scapula (acromion and spine of the scapula) and the clavicle. They binds on the humerus. This muscle is the principal muscle used in the abduction of the arm;

- the pectoralis major muscles originate from the sternum, the ribs and the clavicle and bind to the humerus;

- the latissimus dorsi muscle which takes it origin on the vertebrae, on the illiac crest and on the scapula and insert on the humerus. This muscle is responsible for different mouvement like extension, adduction, flexion and internal rotation;

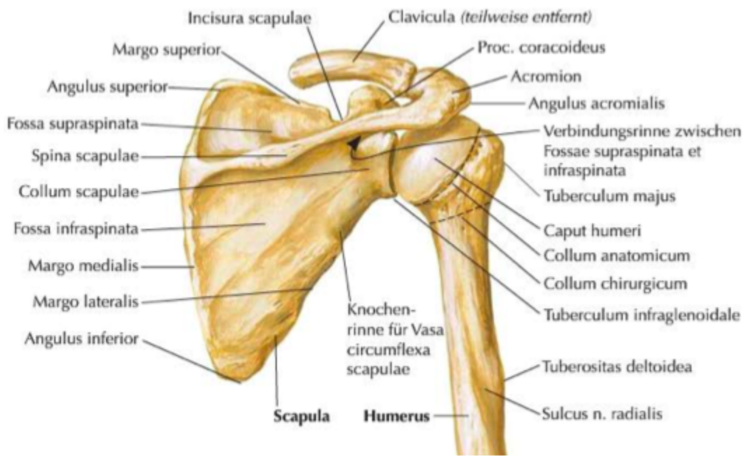

Figure 2.1: Netter, "Atlas of Human Anatomy" 2011

- and the muscles of the rotator cuff which also give the stability to the glenohumeral joint.

Rotator Cuff

The rotator cuff is a group of four muscles that provide stability to the glenohumeral joint and helps other muscles in arm movements. It includes the infraspinatus muscle, the teres minor muscle, the subscapularis muscle and the supraspinatus muscle as we can see in figure 2.2. All these muscle originate from the scapula and their tendons binds on the humerus head, forming the rotator cuff tendon on the humerus.

The infraspinatus with the teres minor are responsible for external rotation and the subscapularis is responsible for internal rotation.

Supraspinatus

The supraspinatus muscle originate from the supraspinatus fossa of the scapula, and its tendon bind on the greater tubercle of the humerus. This muscle works with the deltoid to abduct the shoulder and maintains the humerus in the glenoid cavity of the scapula. The structure of the muscle is pennate, which means that the muscle fiber are not all parallel to each other and are organised in a complex way. Each fiber is attached at a specific angle, the pennation angle, which is described by Kim (2009) "as the acute angle that a muscle fiber bundle creates with the line of force". The supraspinatus tendon fibers are all parallel to each other. They originate on the humerus and are inserted in the muscle.

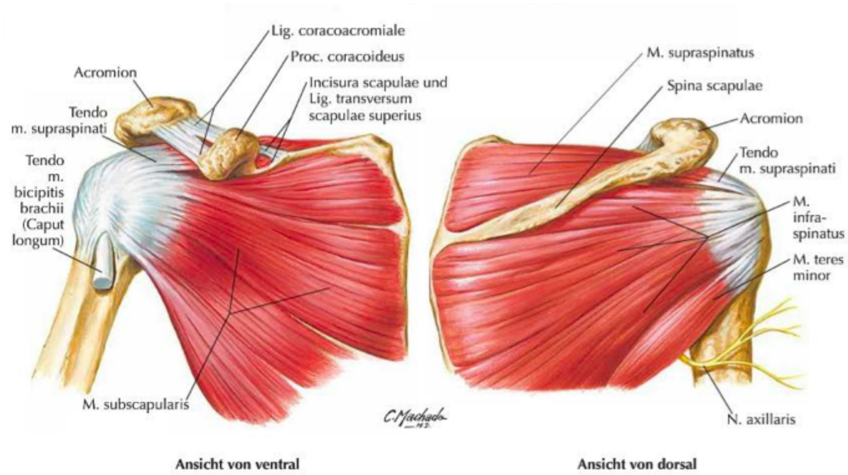

Figure 2.2: Netter, "Atlas of Human Anatomy" 2011

2.2 Pathologies in supraspinatus

The supraspinatus is subject to a lot of tension and is therefore the most vulnerable muscle of the rotator cuff. Muscle pathologies can come from an injury resulting in a tear or from a muscle degradation.

Symptomatology

A rotator cuff tear can be due to degeneration or fatigue of the tendon fibers or can happen after a trauma. The traumatic tear happens after a forcefully raise of the arm against resistance and affects the supraspinatus tendon. Such a tear can result in symptoms like severe pain that radiate through the arm and difficulties lifting the arm. Tears due to degeneration or fatigue happen with repeated overhead activities (like ball throwing) but can also be a consequence of shoulder tendinitis (inflammation of the tendon) or rotator cuff disease (resulting in a inflammation and swelling). The symptoms are a gradually increasing pain and difficulties moving the arm. When the tear is total, the arm can't be lifted forward or outward anymore. (S.C.O.I, 2014)

Pathogenesis

Rotator cuff tears can be partial or full thickness tears. In partial tears, the tendon is not fully torn by opposition of the full thickness tear where the tendon is torn "through-and-through" (Wikipedia, 2014). Tendon tears in the supraspinatus usually happens at the point of insertion of tendon on the humeral head, as it is subject to a lot of tension. A rotator cuff tear can result in muscle atrophy. A muscle atrophy is a reduction of the muscle fiber size and can lead to a fatty acid infiltration. The muscle atrophy is usually a consequence of relieving postures.
Rotator cuff tendinitis is caused by irritation and inflammation of the tendons of the

rotator cuff muscles due to repetitive movements, especially movement over the head (Wright, 2012). Rotator cuff disease includes "impingement syndrome" which is an inflammation of the tendon and a swelling of the bursa. It occurs when the space under the acromion for the supraspinatus muscle to pass is too narrow. This result in a compression of the muscle and the bursa (lubrificating tissus) which will swell and become inflamed. (S.C.O.I, 2014)

Diagnosis

The diagnosis starts with a patient history of activities and symptoms. The symptoms are examined physically with palpation, range of motion and strength testing (Wikipedia, 2014). A more detailed investigation can be made using X-rays, ultrasound scans or MRI (magnetic resonance imaging) scan. Such scans allows to see the anatomy of the bones, muscle atrophy or if there is a tear in the rotator cuff tendon.

Treatement

Tears can be treated surgically but a non-surgical treatment is usually done before, especially in patient whose shoulder function is reasonably maintained. The non-surgical treatment consist of pain relief medication with anti-inflammatories substances, ice packs, physiotherapy and rest. The same non surgical treatment is used in case of "impingement syndrome" and tendonitis. When the non-surgical treatment doesn't work or when the tear is too important a surgical treatment is needed. Surgery repairs depends on the pathology. In case of "impingement syndrome" a subacromial decompression can be made by removing a small part of the acromion (bone). In case of a large tear, tissue suture is necessary. When the tendon is too weak for suture, collagen or other material can be used to reinforce the tendon. (Wikipedia, 2014)

2.3 Simulation of the tendon

2.3.1 Simulation methods

The tendon and the bones have been simulated using the finit element method on Abaqus and Matlab.

Finit Element Method

The finite element method is widely used in engineering and one of the standard tools for deformation analysis on solid bodies. This method consists of dividing the object of interest (here the tendon and the bones) in small subdomaines, which are each represented by a set of element equations to the problem. This subdivision allows an accurate representation of complex geometries and allows to include different material properties. All sets of equation are then recombined into a global system of equation for calculation, which can be solved using numerical iterative algorithms. (Wikipedia, 2014)

Abaqus .inp files

Abaqus .inp files are the output of the Abaqus preprocessor and serve as input for the solver. These files contains the description of the simulated object. In figure 2.3, we can see the input file from a cube divided in tetrahedrons. In the section "*Node" of the file, the definition of the finite element mesh is shown. It contains the position of the nodes in 3D coordinated followed by the assignments of the nodes to the finite elements, in the section "*Element, type=C3D10". Each tetrahedral element is described by 10 nodes, one in each corner of the tetrahedron and one in the middle of each edge.
In the "*MATERIALS" section, specific material properties can be given to each element. The "*User Material, constant=8" section will be modified to introduce the direction of the fiber. The first three number in this section represent the direction of the fiber followed by the properties.

2.3.2 Implementation of fibers

Muscle fibers can be simulated using different methods. The method described by Lu et al. (2011) uses the non-uniform rational B-spline (NURBS) and the finit element method (FEM). "The basic idea of the FEM–NURBS method is to use the NURBS solid for representing the muscle fibre orientation arrangement, and then pass the fibre direction at each Gauss point into the FE model as the initial fibre direction" as showed in figure 2.4. This method allows to draw precisely a fixed number of fibres through a solid model. An other method is described by Blemker and Delp (2004). Their method consists of a simple shape meshing, like a cube, followed by a coordinate transformation to project the cube in the solid section. The solid section is first modelled using the 3D finit element method and the origin and insertion of each muscle were defined as fixed to the bone. This method is illustrated in figure 2.5. This model again has a fixed number of fibres and describes the overall directions of the fibres in the muscle. The last model studied was developed by Choi and Blemker (2013). This method is using a "Laplacian Vector Field Simulation". They are using the fact that "Although the fiber cells typically do not have the length to span the entire muscle, they are grouped in parallel bundles called fascicles, which run between the proximal and distal sites where the muscle attaches to tendon structures or to bones." This means that each muscle is described by an origin and an insertion area and all fascicles never cross each other. By using the "Laplacian Vector Field" they have been able to simulate the distribution of the fiber bundles between the two surfaces (origin and insertion). The result of the simulation in some muscle can be seen in figure 2.6.

```
*Heading
** Job name: Job-1 Model name: Model-1
** Generated by: Abaqus/CAE 6.13-3
*Preprint, echo=NO, model=NO, history=NO, contact=NO
**
** PARTS
**
*Part, name=Part-1
*Node
      1,           1.,           1.,           1.
      2,           1.,           0.,           1.
      3,           1.,           0.,           0.
      4,           1.,           1.,           0.
      5,           0.,           0.,           1.
      6,           0.,           0.,           0.
      7,           0.,           1.,           0.
      8,           0.,           1.,           1.
      9,  0.492907375,  0.533767402,  0.547177196
     10,          0.5,           0.,           1.
     11,           0.,           0.,          0.5
     12,          0.5,           0.,          0.5
     13,  0.246453688,  0.266883701,  0.273588598
     14,  0.746453702,  0.266883701,  0.773588598
     15,  0.246453688,  0.266883701,  0.773588598
     16,           0.,          0.5,           0.
     17,  0.246453688,  0.766883731,  0.273588598
     18,           0.,          0.5,          0.5
     19,           0.,           1.,          0.5
     20,  0.246453688,  0.766883731,  0.773588598
     21,           0.,          0.5,           1.
     22,          0.5,          0.5,           0.
     23,          0.5,           0.,           0.
     24,  0.746453702,  0.266883701,  0.273588598
     25,           1.,           1.,          0.5
     26,  0.746453702,  0.766883731,  0.773588598
     27,  0.746453702,  0.766883731,  0.273588598
     28,          0.5,           1.,          0.5
     29,          0.5,           1.,           1.
     30,           1.,          0.5,           0.
     31,           1.,          0.5,          0.5
     32,          0.5,           1.,           0.
     33,           1.,           0.,          0.5
     34,           1.,          0.5,           1.
     35,          0.5,          0.5,           1.
*Element, type=C3D10
 1,  2,  6,  5,  9, 12, 11, 10, 14, 13, 15
 2,  9,  6,  5,  7, 13, 11, 15, 17, 16, 18
 3,  7,  9,  8,  5, 17, 20, 19, 18, 15, 21
 4,  6,  7,  9,  3, 16, 17, 13, 23, 22, 24
 5,  4,  9,  1,  8, 27, 26, 25, 28, 20, 29
 6,  3,  4,  9,  1, 30, 27, 24, 31, 25, 26
 7,  3,  7,  9,  4, 22, 17, 24, 30, 32, 27
 8,  3,  9,  2,  1, 24, 14, 33, 31, 26, 34
 9,  5,  9,  8,  2, 15, 20, 21, 10, 14, 35
10,  9,  2,  1,  8, 14, 34, 26, 20, 35, 29
11,  6,  9,  2,  3, 13, 14, 12, 23, 24, 33
12,  7,  9,  4,  8, 17, 27, 32, 19, 20, 28
*End Part
*Nset, nset=Set-1, generate
  1,  35,   1
*Elset, elset=Set-1, generate
  1,  12,   1
** Section: Section-1
*Solid Section, elset=Set-1, material=Muscle
,
*End Part
**
**
** ASSEMBLY
**
*Assembly, name=Assembly
**
*Instance, name=Part-1-1, part=Part-1
*End Instance
**
*Nset, nset=Set-1, instance=Part-1-1
  5,  6,  7,  8, 11, 16, 18, 19, 21
*Elset, elset=Set-1, instance=Part-1-1
 2, 3
*Nset, nset=Set-2, instance=Part-1-1
  1,  2,  3,  4, 25, 30, 31, 33, 34
*Elset, elset=Set-2, instance=Part-1-1
 6, 8
*End Assembly
**
** MATERIALS
**
*Material, name=Muscle
*Depvar
      3,
*User Material, constants=8
10.,    0.,    0., 0.227, 3.588,    1.,  0.95,   10.
**
** BOUNDARY CONDITIONS
**
** Name: Fix Type: Symmetry/Antisymmetry/Encastre
*Boundary
Set-1, PINNED
** ----------------------------------------------------------------
**
** STEP: Step-1
**
*Step, name=Step-1, nlgeom=YES
*Static
0.1, 1., 1e-05, 1.
**
** BOUNDARY CONDITIONS
**
** Name: Disp Type: Displacement/Rotation
*Boundary
Set-2, 1, 1, 0.1
**
** OUTPUT REQUESTS
**
*Restart, write, frequency=0
**
** FIELD OUTPUT: F-Output-1
**
*Output, field, variable=PRESELECT
**
** HISTORY OUTPUT: H-Output-1
**
*Output, history, variable=PRESELECT
*End Step
```

Figure 2.3: Abaqus input file for a cube divided in tetrahedons

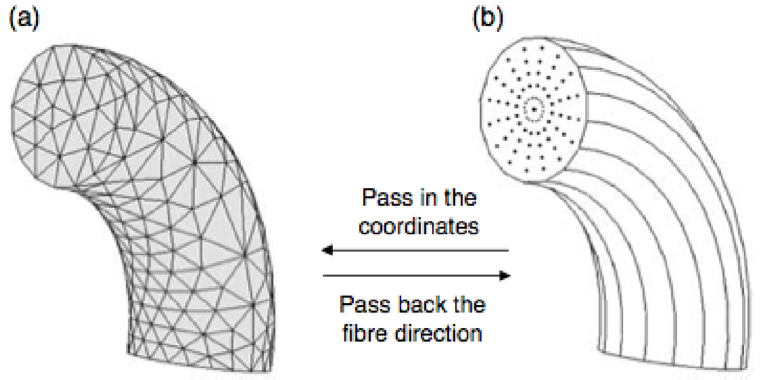

Figure 2. Illustration of the FEM−NURBS method: (a) FE model with tetrahedrons and (b) NURBS solid model with the fibre orientation arrangement indicated.

Figure 2.4: Lu and al., '"Modelling skeletal muscle fibre orientation arrangement" 2011

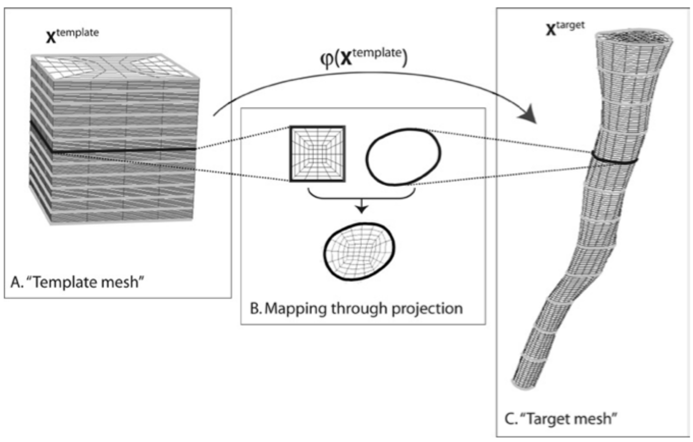

FIGURE 3. Creation of volumetric meshes of each muscle from segmented surface models. Hexahedral meshes were created by mapping a "template" hexahedral mesh (A) through a series of projections (B) to the "target" mesh (C). Each slice of the mesh corresponds to an outline of an anatomical structure created during segmentation (see Fig. 2).

Figure 2.5: Blemker and Delp, "Three-Dimensional Representation of Complex Muscle Architectures and Geometries" 2004

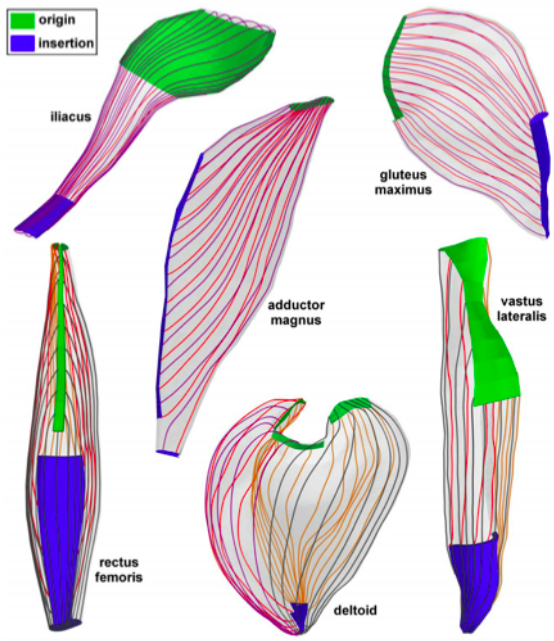

Figure 4. Generated fascicle trajectories in 3D anatomical examples of skeletal muscles. In each muscle, the origin (proximal) and insertion (distal) attachment regions are shown in green and blue respectively. For sake of visibility, only samplings of fascicle tracts on the muscle surface are shown. The different colors of the fascicle tracts are only for purpose of visual contrast.
doi:10.1371/journal.pone.0077576.g004

Figure 2.6: Choi and Blemker, "Skeletal Muscle Fascicle Arrangements Can Be Reconstructed Using a Laplacian Vector Field Simulation" 2013

3 Methods

3.1 Simulation model

An existing model of the glenohumeral joint was used. This model was created using the finit element method and includes two bones: the scapula and the humerus, and the supraspinatus muscle tendon, as shown in figure 3.1 (arm at rest). Two models were used: one with the arm in the rest position (figure 3.1) and one model with the arm in 90 ° abduction. The finit element method is useful here as the supraspinatus tendon fibers have different directions in the whole structure. This method allows then to give a specific fiber direction to each element by modifying the .inp input file, as described in section 2.3.1.
To compare the strain in each models a force was applied on the tendon. In the 90 ° abduction models a force of 60N was applied and in the rest position, a force of 30N was applied. The force was applied on the tendon in the direction of the muscle origin on the scapula fossa. These forces represent the muscular forces which were computed using EMG as described by Engelhardt et al. (2014). These forces were then applied in Abaqus and an Abaqus function was used to show the strain distribution in each model.

3.2 Implementing of the fiber direction in the tendon of the supraspinatus

To implement the direction of the tendon fibers on the three dimensional model, Bezier curves and Spline curves have been used. These curves describe the general direction of the fiber which has then been applied to the finit elements. The orientation of the fibers in the tendon was studied in both positions: 90 ° abduction and rest position.

3.2.1 Abduction position

The fibers in the tendon were simulated in a contracted state (arm at 90 °). The simulation of the tendon was performed in Abaqus and the coordinates of the nodes was extracted in an .inp file to be used in Matlab. In the abducted position, all the fiber in the tendon are in the same direction. I attributed that direction to each element and simulated the vector field.

3.2.2 Rest position

A second simulation was done in the resting position, which means with the arm along the body. In this position, the tendon follows the curvature of the humeral head and the fibers are therefore no longer in the same direction in each element. The element informations where extracted from the Abaqus simulation in an .inp file and the fiber direction were determined using Matlab. To simulate the curvature of the tendon two methods were tested: a Bézier curve fitting and a Spline curve fitting method.

Bézier curve

A Bézier curve is created using a set of control point through which a curve is fitted as shown in figure 3.2. A cubic Bézier curve was used. The curve start at point P_0, goes toward point P_1 and then P_2 and ends at point P_3. It is described by the following equation:

$$B(t) = P_0(1-t)^3 + 3P_1t(1-t)^2 + 3P_2t^2(1-t) + P_3t^3 \ , \ t \in [0,1].$$

This equation was used to compute a curve in 3 dimensions to best fit the tendon shape. P_0, P_1, P_2 and P_3 where selected on the Abaqus simulation of the tendon. The curve was simulated in Matlab.

Spline curve

A spline curve can be described as an interpolation of points between known points. The spline curve will then pass through all the fixed points, as shown in figure 3.3 by opposition to the Bézier curve. The curve was interpolated using a 3 dimensional cubic cardinal spline curve (or Catmull-Rom spline) using Khan (2005) Matlab method. Six fixed points were selected on the surface of the tendon. The Catmull-Rom spline is an interpolation of a curve between 2 points using the previous and the next point on the spline. The curves are given by the following equation as described by Twigg (2003):

$$p(s) = \begin{bmatrix} 1 & u & u^2 & u^3 \end{bmatrix} \begin{bmatrix} 0 & 1 & 0 & 0 \\ -\tau & 0 & \tau & 0 \\ 2\tau & \tau-3 & 3-2\tau & -\tau \\ -\tau & 2-\tau & \tau-2 & \tau \end{bmatrix} \begin{bmatrix} p_{i-2} \\ p_{i-1} \\ p_i \\ p_{i+1} \end{bmatrix} \ , \ u \in [0,1]$$

Where the parameter τ is the "tension", which defines how sharp the curve bends and is set to 1/2. This formula was then used to interpolate the curve between each selected points. For the interpolation between the first two points: p_0 and p_1 the previous point was set to the same point as p_0 and the next point is p_2. The same was done for the last two points, the next point was set to be the same as the last point. The number of points used to describe the curve in between each set of points was set to 100.

Simulation of the fibers in the tendon

The fibers directions were then simulated in each finit element. The direction was given by the tangent direction from the nearest point on the curve from the center of each element (i.e the point on curve on the same cross section as the point of interest) to the next point on the same curve (Bézier or spline curve), as shown in figure 3.4. A direction vector field was then created at the center of each element following the attributed direction vectors.

Comparison between Bezier and Spline curves

To have a better view of the differences in fiber direction using Bezier curve or the Spline curve, a comparison was done. To do so, the difference between both direction vectors (the one from the Bezier interpolation and the one from the Spline curve interpolation) were computed. A distance difference threshold was fixed and both vectors were plotted when the difference between them was higher than the threshold. Different threshold values were tested and the most significant one was used to show the comparison.

Final model

Once the Matlab simulation was done, a new .inp file was created. This new file is a copy of the original file but with in addition the fiber direction for each element and each element's material was defined separately. This new file was then run in Abaqus.

3.3 Tendon Material Definition

To be able compare the anisotropic model with an isotropic model, two different material properties had to be defined:

- Isotropic case: the exponential isotropic law was used. The material properties was defined as the average properties in all direction of the tendon. The material properties used in the .inp files were modified the following way:

  *User Material, constants=8

  1, 0., 0., 1.227, 14.18, 0.001, 1., 1.

  **

- Anisotropic case: the exponential transverse isotropic law was used. The material properties were identified in fiber direction and in the transverse plane. The material properties were defined for each element in the following way:

  *Material, name=Tendon1

  *Depvar

  3,

  *User Material, constants=8

  0.382194, 0.374489, 0.844799, 1.227, 14.18, 0.001, 0.7175, 1.

  As described by Ehret and al (2011). The first three values describe the fiber direction and were given by the direction interpolated using the spline curve as described in section 3.2.1.

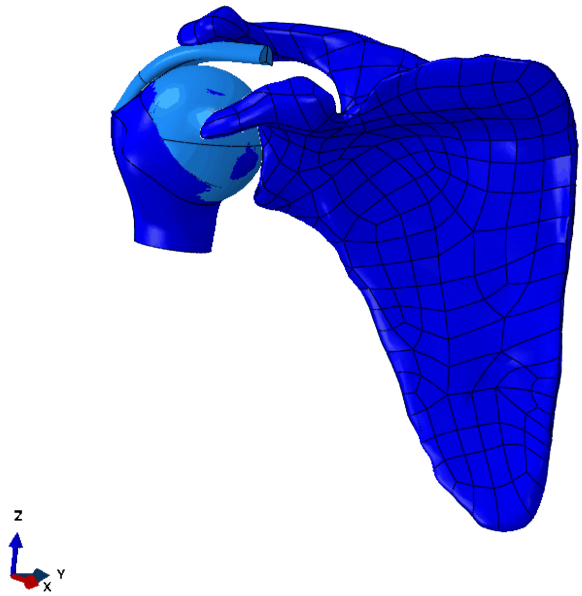

Figure 3.1: Model used to simulate the fiber in the resting position showing the humeral head, the tendon and the scapula.

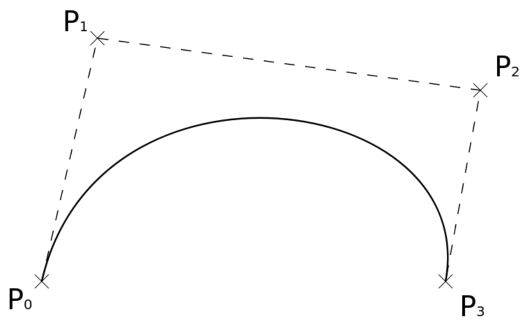

Figure 3.2: Cubic Bézier curve

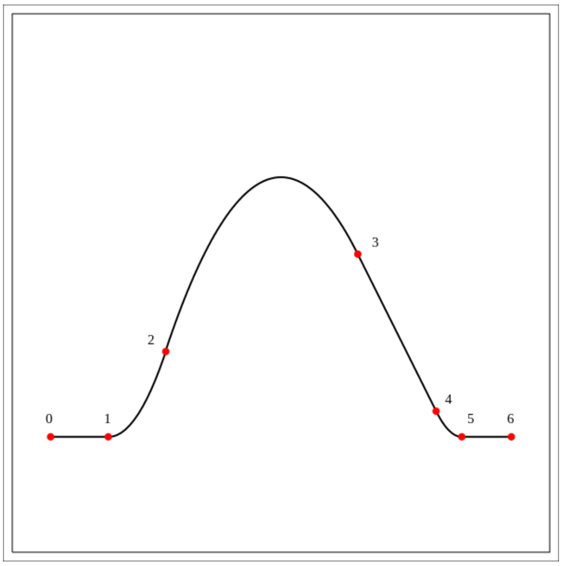

Figure 3.3: Quadratic Spline curve

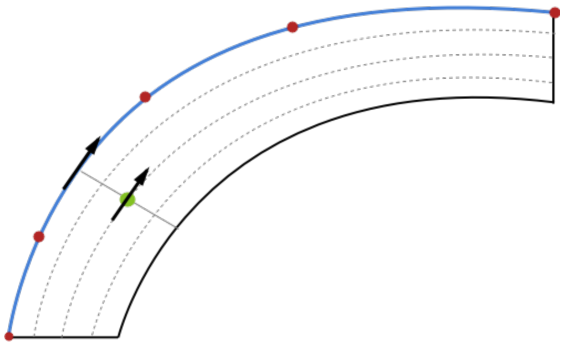

Figure 3.4: Attribution of the fiber direction given by the direction of the curve on the same cross section. In blue: Spline curve following the shape of the tendon; red dots: points used to create the spline curve; arrows: fiber direction on a same cross section applied to the green dot.

4 Results

4.1 Fiber direction in the supraspinatus tendon in the abducted position

The fiber direction in the 90 ° abduction position is shown in figure 4.1. All the fibers are parallel and in the same direction.

4.2 Fiber direction in the supraspinatus tendon in rest position

4.2.1 Bézier curve

The interpolation of the fiber direction using a Bezier curve as described in section 3.2.2 is shown in figure 4.2. The curve follows approximatively the centerline of the tendon.

4.2.2 Spline curve

The interpolation of the fiber direction using a spline curve as described in section 3.2.2 is shown in figure 4.3. The curve follows the shape of the surface of the tendon. The fiber orientation shows that the fiber follows well the general form of the tendon. A comparison dissection could have been done to confirme the good simulation.

4.2.3 Comparison

These two curves seems to result in a similar fiber orientation in each element. However, the spline curve seems to be a better approximation of the shape of the tendon as it follows well its surface, by opposition of the Bézier curve which doesn't follow the tendon precisely through its midline. In fact, the spline curve is also described by more points (6 points) on the tendon and can therefore follow more precisely the curvature compared to the Bézier curve (only 4 points).
A comparison of the direction of the vector as described in section 3.2.2 is shown in figure 4.4. We can see that the main differences are at both extremities and at the top part of the curvature. At that position, there was no control point for the Bézier curve but there was one for the spline curve interpolation. Therefore, the model using the spline curve was used for further analysis.

4.2.4 Final model

The final model created as described in part 3.2.2, is shown in figure 4.5 in side view. This model shows that the fibers follow the tendon shape. The fibers are all parallel to

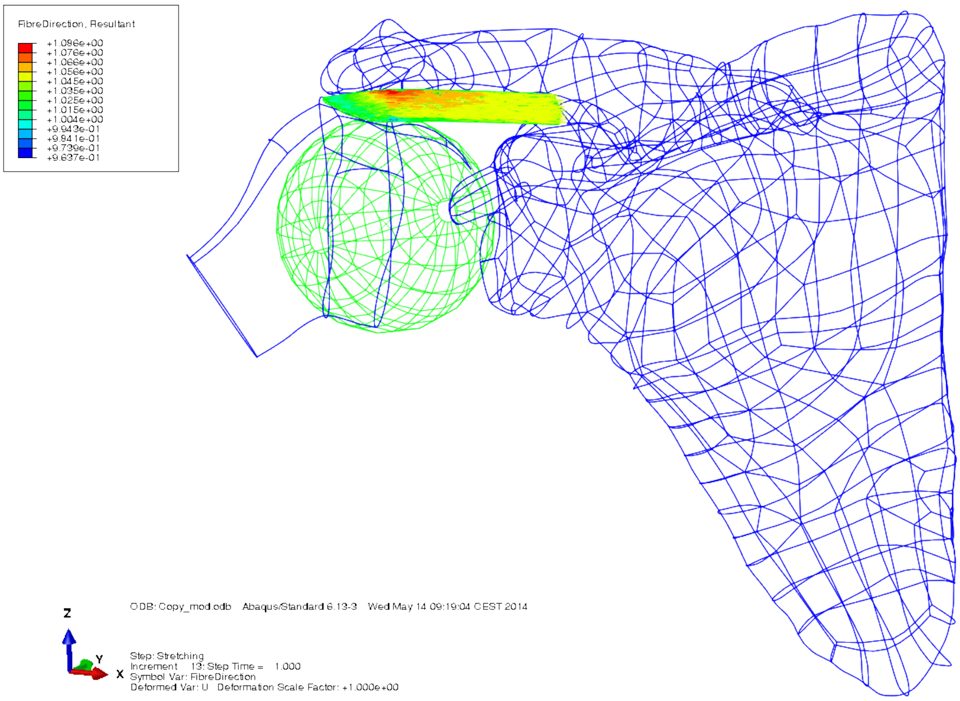

Figure 4.1: Fiber direction in the tendon in the abducted position.

each other from a top view.

4.3 Comparison between anisotropic and isotropic

4.3.1 90 ° abduction

The comparison described in section 3.2 is shown in figure 4.6. The comparison between strain values shows that the strain is higher in the isotropic case, with a value of 0.619 compared to 0.375 in the anisotropic model. The strain in the isotropic case is nearly the double of the strain in the anisotropic case. The position of the maximal strain is the more or less at the same place in both models, on the distal side of the tendon insertion on the humeral head.

4.3.2 Rest position

The comparison described in section 3.2 is shown in figure 4.7. The comparison shows that the maximal strain in the isotropic model is higher, with a value of 0.489 compared to 0.331 in the anisotropic model. The position of the maximal strain is again more or less at the same place in both models, on the distal side of the tendon insertion on the humeral head.

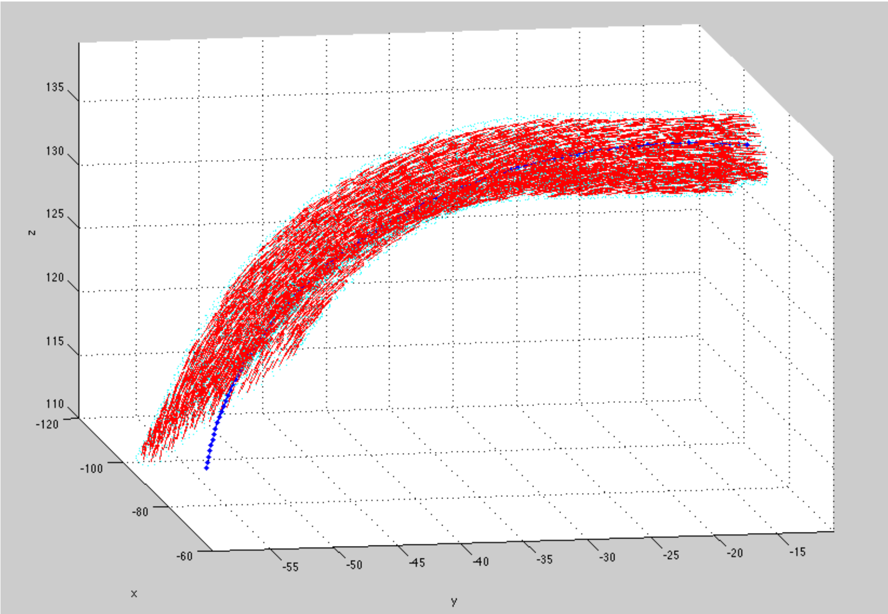

Figure 4.2: Simulation of the fiber directions (red) in the supraspinatus tendon using a Bezier curve (blue), in Matlab.

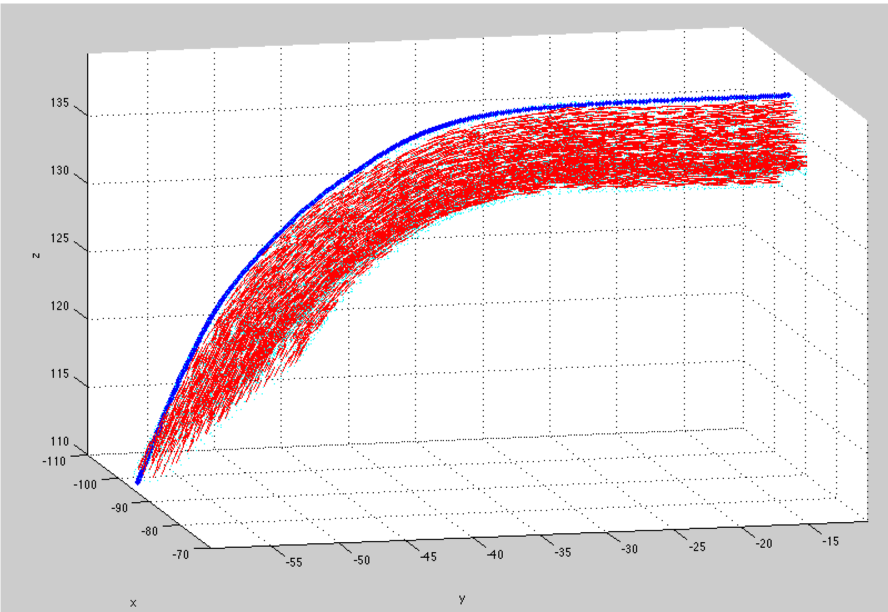

Figure 4.3: Simulation of the fiber directions (red) in the supraspinatus tendon using a Spline curve (blue), in Matlab.

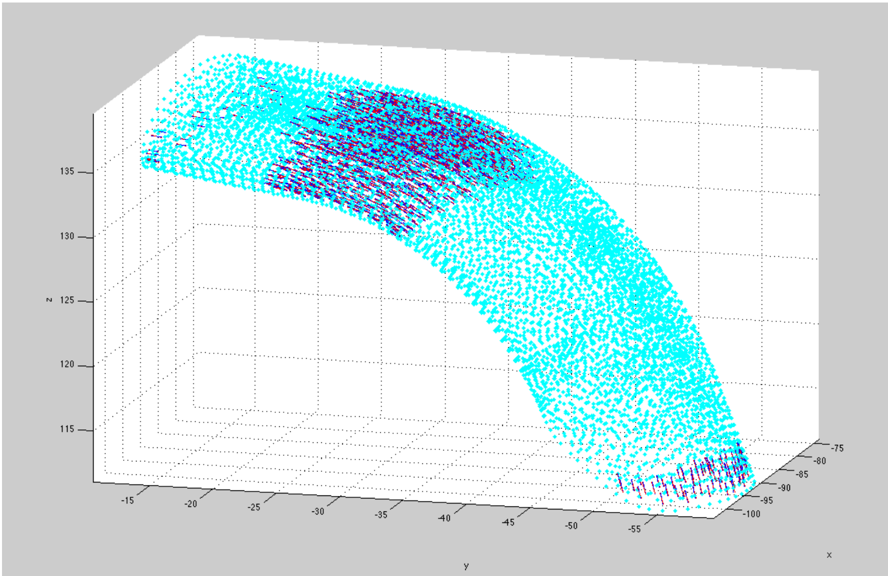

Figure 4.4: Simulation of the comparison between the Bézier interpolation (blue) and the Spline curve interpolation (red) at the important difference points, in Matlab. The nodes are used to simulate the general form of the tendon (cyan).

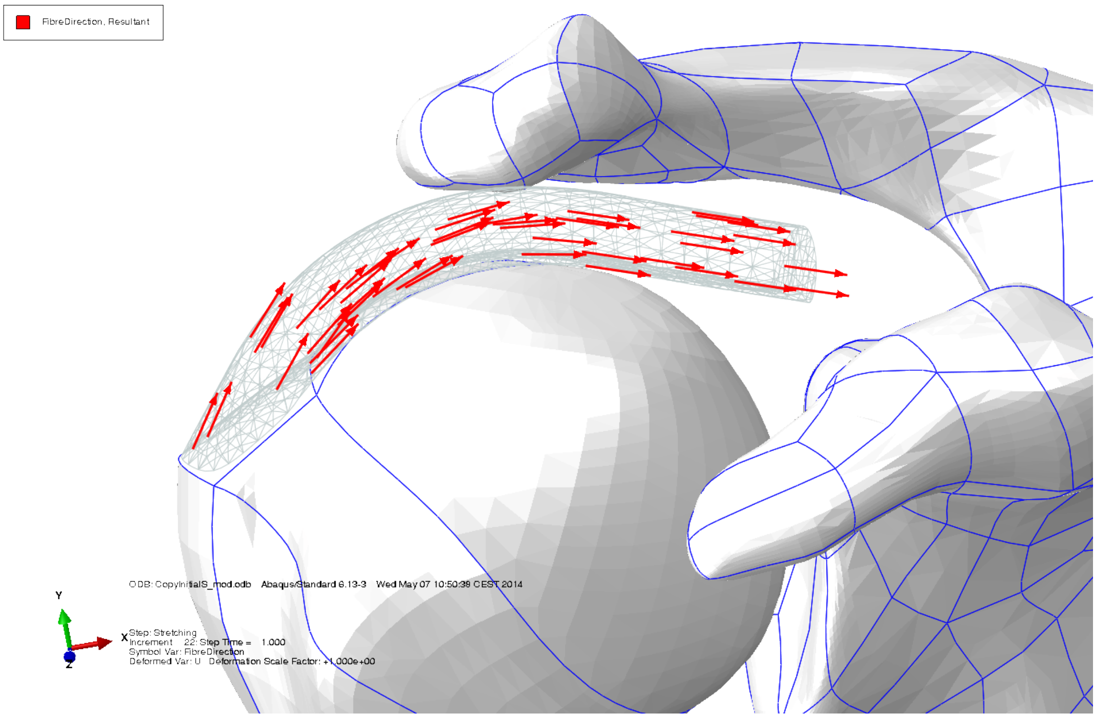

Figure 4.5: Front view of the 3D model (in Abaqus) including fiber directions (red arrows) of the tendon described by a spline curve.

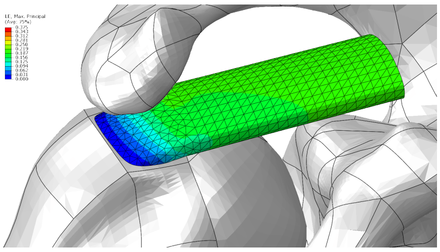

(a) Strain in the anisotropic model, on the surface of the tendon

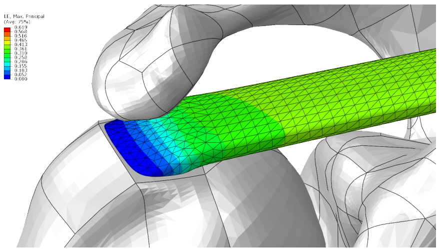

(b) Strain in the isotropic model, on the surface of the tendon.

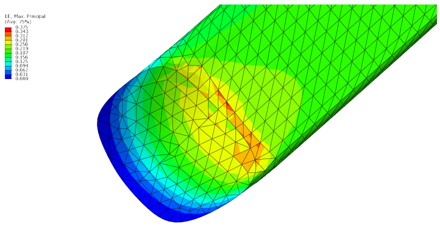

(c) Strain in the anisotropic model, the maximal strain is 0.375, on the distal side of the tendon insertion.

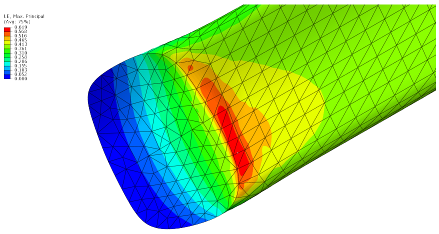

(d) Strain in the isotropic model, the maximal strain is 0.619, on the distal side of the tendon insertion.

Figure 4.6: Comparison between the anisotropic and isotropic models in 90 $^\circ$ abduction position.

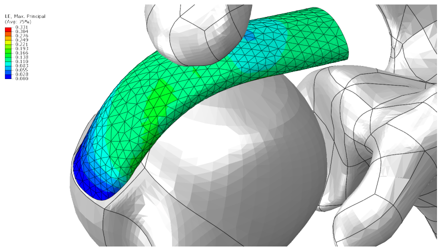

(a) Strain in the anisotropic model, on the surface of the tendon.

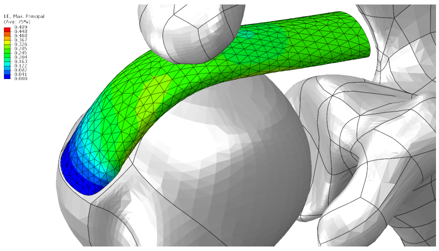

(b) Strain in the isotropic model, on the surface of the tendon.

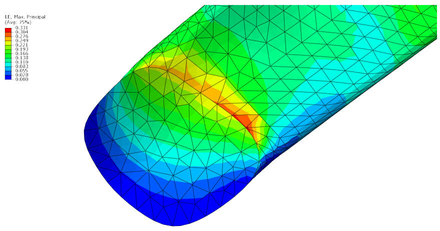

(c) Strain in the anisotropic model, the maximal strain is 0.331, on the distal side of the tendon insertion.

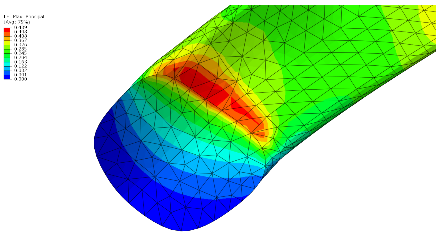

(d) Strain in the isotropic model, the maximal strain is 0.489, on the distal side of the tendon insertion.

Figure 4.7: Comparison between the anisotropic and isotropic models in rest position

5 Discussion and conclusion

The aim of this project, which was to analyse the deformation of the supraspinatus tendon and to compare isotropic vs anisotropic modelling techniques of the tendon tissue, was reached. Fiber direction have been simulated in the model using spline curves and two models using isotropic and anisotropic material have been implemented. This two models have then been compared and showed important differences.

The simulation of the fiber direction resulted in a good model of the supraspinatus tendon. In fact, the fibers are all parallel to each other and perpendicular to the cross section. The spline curve (Catmull-Rom Spline) allowed a better simulation as the curve followed the surface of the tendon and therefore the extrapolated fiber direction were closer to the general form of the tendon. The Bézier curve, even if its simulation was easier, didn't allow a good approximation of the tendon shape. Therefore the fiber direction vector field created using the spline curve was used for the further experiments.

The comparison between the isotropic and the anisotropic model gave the following results. The simulation in both position (90 ° abduction and rest position) showed a higher strain in the isotropic case than in the anisotropic case. In fact, in the isotropic case, the material was defined as the average of the tendon material in all direction and was therefore softer in the fiber direction and stronger in the transverse direction. Therefore, when a force was applied on the isotropic tendon, the deformation was larger than in the anisotropic case where the material was defined in both directions. In both, isotropic and anisotropic case, the position of the maximal strain was at the distal side of the tendon insertion which is consistant with the clinical observation. In fact, the supraspinatus tendon tears, occurs, most of the time, at the insertion of the tendon on the humeral head.
The anisotropic case is therefore supposed to be a better simulation of the tendon as it takes into account the fibrous structure of the tendon.

One positive point in this project was that the interpolation of the fiber direction using the spline curves follows precisely the surface of the tendon. Therefore, a good simulation could be implemented to described the fiber direction and allowed a significative comparison between different models.

An other positive point is that the isotropic model was very simple to simulate as there was no fiber direction to take into account, therefore it also illustrate well the models used in previous studies. The isotropic material properties were given by the average of the material properties in all direction, which is the approximation generally used as it

takes the whole structure of the tendon in consideration.
The anisotropic model, is supposed to be a good representation of the tendon as the fibers follows the general fibrous structure of the tendon with fibers parallel to each other and perpendicular to the cross section. The material was also defined in both direction and gives therefore more consistant results than the isotropic model, as the strength of the fibrous tendon in not the same in the fiber direction than in the transverse plane.
The comparison of the two models could be made easily by comparing the strain in each model.

One weak point of this project was that the implementation of the spline curve was more complicate to simulate than the Bézier curve. The spline curve were selected as they allow to follow precisely the surface of the tendon compared to the Bézier curve which are only an approximation of the middle line of the tendon. Even if the spline curve follows well the surface of the tendon, the model with the interpolated fibers was not compared to reality and is therefore an approximation and supposition of the structure. As it is known that all fibers are parallel and never cross each other, the model can be supposed close to reality as the general form of the tendon, which is given by the fibers, is well followed by the spline curve. The other fiber direction were defined parallel to the spline curve and gives therefore a good approximation of the real fiber direction in the tendon.

An other point that could be improved is the description of the anisotropic material properties. In fact, the anisotropic model was defined with two material properties, one in the fiber direction and one in the transverse direction in the whole tendon. A study from Lake and al. (2009) showed in fact that the material propertied are not the same in different part of the tendon. This irregularity was not taken into account in this project.

To confirme the fiber orientation of the model, an analysis of the fiber directions in the tendon could be done using MRI or ultrasound images or by dissection to confirme if the model used is good or if the model using the Bézier curve still would be better, of if a new model should be created.

To confirme that the anisotropic model is better, a statistical test could be done to show if the difference between the isotropic and anisotropic case are significative. A simulation in the isotropic case could also be done using other material properties, for exemple the properties in the fiber direction could be applied to all direction and compared to the other models. In fact, it still is easier to use an isotropic material definition to simulate this structures and it could be useful to study if it would be possible to find a material property in the isotropic case which would be close enough to an anisotropic simulation.

A better material definition for the anisotropic case could be done using the results of Lake and al. (2009). Different properties could be assigned to the different part of the tendon which would allow to get a model closer to the real tendon structure.

This project allowed to show that the isotropic model of the tendon is not a precise model, and the tendon can be simulated with it's fibrous structure. The creation of a new anisotropic model was done and can now be used for other experiments. This model can still be improved and could then be used to create better model which could help to better understand the mechanical contribution in shoulder pathologies.

Bibliography

Blemker, S. S. and Delp, S. L. 2004. Three-dimensional representation of complex muscle architectures and geometries. Department of Bioengineering and Mechanical Engineering, Stanford University, Stanford, CA.

Choi, H. F. and Blemker, S. S. 2013. Skeletal muscle fascicle arrangements can be reconstructed using a laplacian vector field simulation.

Ehret, A. and al. 2011. A continuum constitutive model for the active behaviour of skeletal muscle.

Engelhardt, C., , Camine, V. M., Ingram, D., Mullhaupt, P., Farron, A., Pioletti, D., and Terrier, A. 2014. Comparison of an emg-based and a stress-based method to predict shoulder muscle forces. URL `http://infoscience.epfl.ch/record/197122?ln=en`.

Khan, M. 2005. N dimensional cardinal spline (catmull-rom) spline interpolation. URL `http://www.mathworks.com/matlabcentral/fileexchange/7326-n-dimensional-cardinal-spline--catmull-rom--spline-interpolation`.

Kim. 2009. Supraspinatus musculotendinous architecture: A cadaveric and in vivo ultrasound investigation of the normal and pathological muscle. University of Toronto.

Lake, S. and al. 2009. Tensile properties and fiber alignment of human supraspinatus tendon in the transverse direction demonstrate inhomogeneity, nonlinearity, and regional isotropy.

Lu, Y. T., Zhu, H. X., Richmond, S., and Middleton, J. 2011. Modelling skeletal muscle fibre orientation arrangement computer methods in biomechanics and biomedical engineering. Computer Methods in Biomechanics and Biomedical Engineering.

Marieb, E. N., 2005. Anatomie et Physiologie humaine. Pearson Education.

Netter, F. H., 2011. Atlas of Human Anatomy.

S.C.O.I, S. C. O. I. 2014. Rotator cuff disease / impingement syndrome. URL `http://www.scoi.com/rotator-cuff.php`.

Twigg, C. 2003. Catmull-rom splines.

Wikipedia. 2014. "shoulder — Wikipedia, the free encyclopedia" "rotator cuff — Wikipedia, the free encyclopedia" "rotator cuff tear — Wikipedia, the free encyclopedia" "supraspinatus muscle — Wikipedia, the free encyclopedia" "finit element method — Wikipedia, the free encyclopedia". http://en.wikipedia.org/wiki/Shoulder/, http://en.wikipedia.org/wiki/Rotator_cuff, http://en.wikipedia.org/wiki/Rotator_cuff_tear, http://en.wikipedia.org/wiki/Supraspinatus_muscle, http://en.wikipedia.org/wiki/Finite_element_method.

Wright, D. M. 2012. Rotator cuff injury and inflammation. URL http://www.patient.co.uk/health/Rotator-Cuff-Injury-and-Inflammation.htm.